



Original article

# Deciphering role of technical bioprocess parameters for bioethanol production using microalgae

Farhana Bibi<sup>a</sup>, Humaira Yasmin<sup>b</sup>, Asif Jamal<sup>a</sup>, Mohammad S. AL-Harbi<sup>e</sup>, Mushtaq Ahmad<sup>c</sup>, Muhammad Zafar<sup>c</sup>, Bashir Ahmad<sup>d</sup>, Bassem N. Samra<sup>e</sup>, Atef F. Ahmed<sup>e</sup>, Muhammad Ishtiaq Ali<sup>a,\*</sup><sup>a</sup> Department of Microbiology, Quaid-i-Azam University, Islamabad, Pakistan<sup>b</sup> Department of Biosciences, COMSATS University Islamabad (CUI), Islamabad, Pakistan<sup>c</sup> Department of Plant Sciences, Quaid-i-Azam University, Islamabad, Pakistan<sup>d</sup> Department of Biotechnology, International Islamic University, Islamabad, Pakistan<sup>e</sup> Department of Biology, College of Science, Taif University, P.O. Box 11099, Taif 21944, Saudi Arabia

## ARTICLE INFO

### Article history:

Received 26 August 2021

Revised 3 October 2021

Accepted 4 October 2021

Available online 11 October 2021

### Keywords:

Microalgae  
Biomass productivity  
Specific growth rate  
Optimization  
RSM  
Bioethanol

## ABSTRACT

Microalgae biomass is considered an important feedstock for biofuels and other bioactive compounds due to its faster growth rate, high biomass production and high biomolecules accumulation over first and second-generation feedstock. This research aimed to maximize the specific growth rate of fresh water green microalgae *Closteriopsis acicularis*, a member of family *Chlorellaceae* under the effect of pH and phosphate concentration to attain enhanced biomass productivity. This study investigates the individual and cumulative effect of phosphate concentration and pH on specific growth characteristics of *Closteriopsis acicularis* in autotrophic mode of cultivation for bioethanol production. Central-Composite Design (CCD) strategy and Response Surface Methodology (RSM) was used for the optimization of micro-alga growth and ethanol production under laboratory conditions. The results showed that high specific growth rate and biomass productivity of  $0.342 \text{ day}^{-1}$  and  $0.497 \text{ g L}^{-1} \text{ day}^{-1}$  respectively, were achieved at high concentration of phosphate ( $0.115 \text{ g L}^{-1}$ ) and pH (9) at 21st day of cultivation. The elemental composition of optimized biomass has shown enhanced elemental accumulation of certain macro (C, O, P) and micronutrients (Na, Mg, Al, K, Ca and Fe) except for nitrogen and sulfur. The Fourier transform infrared spectroscopic analysis has revealed spectral peaks and high absorbance in spectral range of carbohydrates, lipids and proteins, in optimized biomass. The carbohydrates content of optimized biomass was observed as 58%, with  $29.3 \text{ g L}^{-1}$  of fermentable sugars after acid catalyzed saccharification. The bioethanol yield was estimated as 51 % g ethanol/g glucose with maximum of 14.9 g/L of bioethanol production. In conclusion, it can be inferred that high specific growth rate and biomass productivity can be achieved by varying levels of phosphate concentration and pH during cultivation of *Closteriopsis acicularis* for improved yield of microbial growth, biomass and bioethanol production.

© 2021 The Authors. Published by Elsevier B.V. on behalf of King Saud University. This is an open access article under the CC BY-NC-ND license (<http://creativecommons.org/licenses/by-nc-nd/4.0/>).

\* Corresponding author.

E-mail addresses: [humaira.yasmin@comsats.edu.pk](mailto:humaira.yasmin@comsats.edu.pk) (H. Yasmin), [asifjamal@qau.edu.pk](mailto:asifjamal@qau.edu.pk) (A. Jamal), [mushtaq@qau.edu.pk](mailto:mushtaq@qau.edu.pk) (M. Ahmad), [zafar@qau.edu.pk](mailto:zafar@qau.edu.pk) (M. Zafar), [bashir.ahmad@iiu.edu.pk](mailto:bashir.ahmad@iiu.edu.pk) (B. Ahmad), [ishimri@qau.edu.pk](mailto:ishimri@qau.edu.pk) (M.I. Ali).

Peer review under responsibility of King Saud University.



## 1. Introduction

Continuous crises in energy sector due to depletion and unsustainability of fossil reserves, climate changes associated with use of petro derived fuels and auxiliary environmental risks leads the attention of research towards green, sustainable and ecofriendly alternatives of fossil fuels (Ameen et al., 2021; Kim et al., 2021). Microalgae biomass is considered an important alternative tiny reserves of bioactive compounds with significant potential of producing biofuels (Khan et al., 2018). Bioethanol production and application as green fuel has been rising in the world (Chakraborty & Mukhopadhyay, 2020). The major raw materials being used at industrial scales for the bioethanol production

<https://doi.org/10.1016/j.sjbs.2021.10.011>

1319-562X/© 2021 The Authors. Published by Elsevier B.V. on behalf of King Saud University.

This is an open access article under the CC BY-NC-ND license (<http://creativecommons.org/licenses/by-nc-nd/4.0/>).

belongs to first and second generation feed stocks, such as sugar cane and cereals owing to the higher level of fermentable sugars and total carbohydrates contents (Bušić et al., 2018). However, the cultivation of feed stock crops requires huge arable land and results in slower growth of plants, which poses major challenges in the progress of bioethanol production. Conversely, microalgae is an attractive substitute of the traditional materials due to preferentially high productivity, faster growth rates, less land requirements, less harvesting time and simple nutrients requirement for its growth (Özçimen & İnan, 2015). In general, microalgal strains with faster growth rate and high biomass productivity are desired potential candidates for biofuel production. Strain such as *Chlorella vulgaris* (family *Chlorellaceae*) and *Chlamydomonas reinhardtii* (family *Chlamydomonadaceae*) are reported with potential to produce up to 3.28 g L<sup>-1</sup> and 0.86 g L<sup>-1</sup> of biomass per day which offers them as a suitable candidate for biofuel production (Metsoviti et al., 2019; Sankaran et al., 2018). However, slower growth rate and less biomass production are still challenges in large-scale production and plays decisive role in the commercialization of microalgae-derived biofuels. Such potential strains have already been used in many countries as fraction and blends of petro fuels (Turkcan, 2018; Yusuf & Inambao, 2021). Strains isolated from USA or other regions of world are not suitable to cultivate for higher production in Pakistan due to remarkable difference in seasonal and environmental variations. In order to ensure better adaptability to environmental factors for high biomass productivity, it is desired to isolate local indigenous microalgal strains that grow best in natural and regional habitat (Gill et al., 2016).

Algal cells are mainly rich source of lipids, carbohydrate, proteins and other value added products (Özçimen & İnan, 2015). Several algal species rich in total carbohydrates such as; *Chlorella* sp. (77.6%) and *Scenedesmus* sp. (58.6%) are reported in previous studies, suitable for biofuel production (Do et al., 2021). Being rich in cellulosic content, Algal biomass offers advantage over other biofuel feedstock's as, biochemically algal cells lacks hemicellulose and lignin, which simplifies the process of bioethanol production (Özçimen & İnan, 2015). The dominant algal genera; *Chlorella*, *Chlamydomonas*, *Scenedesmus*, *Chlorococcum* are reported for enhanced biomass and carbohydrates content (Fozer et al., 2019; Metsoviti et al., 2019; Özçimen & İnan, 2015). Biochemical composition of microalgae could be altered and improved by changing abiotic growth conditions such as; salinity, temperature, light intensity, pH, and nutrient concentration (Almutairi et al., 2021; Kurano & Miyachi, 2005; Zhang et al., 2019). Among these cultivation parameters, pH and phosphate concentration are important factors affects the algal growth and biomass productivity (Almutairi et al., 2020; Feng et al., 2012; Poh et al., 2020; Yun et al., 2014). Variation in pH is associated with growth and accumulation of microalgal biomass in several ways. It mainly affects the carbon distribution and availability to species, changes the accessibility of trace metals and nutrients by causing direct physiological effects (Chen & Durbin, 1994; Suthar & Verma, 2018). Phosphate concentration affects the division and growth of algal cells by playing important role in energy transport, membrane formation, storage and replication of genetic information (Liu et al., 2021).

Recently, the optimization of algal cultivation conditions to attain rapid growth rate and enhanced accumulation of required biomolecules has gained considerable attention (Khan et al., 2018; Miranda et al., 2016). Generally, algal biomass productivity in large-scale facilities is restricted to species, which are adapted to high pH and salt concentration and able to overcome naturally occurring contaminants. Hence, optimization of pH and salt concentration confers competitive advantage over undesirable microorganisms and decreases production cost of biomass by

increasing productivity (Phwan et al., 2018). Although, there are number of microalgae strains isolated and characterized for their biochemical composition and biofuel potential, the isolation and characterization of indigenous strains that offers better adaptability to natural environment are still important for sustainable and environment friendly biofuels production (Joe et al., 2018).

In present study, an indigenous fresh water green microalgae *Closteriopsis acicularis* was isolated and characterized for high specific growth rate and biomass productivity with aim to be used as bioethanol feedstock. The effect of phosphate concentration and pH were examined and optimized for faster growth rate and biomass productivity. To the best of our insight, this strain is not disclosed for its growth characterization and optimization studies. There is less information available regarding physiology and biochemistry of this strain in literature reported. In order to get insight of physiological and biological traits of this strain, response surface method (RSM) was utilized along with factorial design of experiment to study the independent and interactive effect of pH and phosphate concentration on growth rate and biomass productivity of this strain. Bioethanol yield was estimated following acid catalyzed saccharification and yeast (*Saccharomyces cerevisiae*) based fermentation of optimized biomass.

## 2. Materials and method

### 2.1. Sampling collection

Fresh water microalgae samples were collected from Rawal lake Islamabad (Climate humid subtropical, temperature 30 °C, pH 8.1) with the aim of isolation and identification of potential strain capable of faster growth rate and biomass productivity. 100 ml of sterile falcons tubes were used to collect sample and samples were stored in falcon tubes at 4 °C.

### 2.2. Growth conditions

Streak plate method was used for isolation of algal strain in modified BBM media with 1.5% agar. In order to avoid any fungal or bacterial contamination, an antibacterial (Ampicillin) and anti-fungal (Carbendazim) concentration of 0.1 µg/ml each is added to enrichment media prior to sample transfer (Mustapa et al., 2016). The modified BBM media was composed of chemical components in g/L dist-H<sub>2</sub>O as; NaNO<sub>3</sub>, 0.25; CaCl<sub>2</sub>, 0.025; MgSO<sub>4</sub>, 0.075; K<sub>2</sub>HPO<sub>4</sub>, 0.075; KH<sub>2</sub>PO<sub>4</sub>, 0.175; NaCl, 0.025; EDTA, 0.05; KOH, 0.31; FeSO<sub>4</sub>·7H<sub>2</sub>O, 0.049; H<sub>3</sub>BO<sub>3</sub>, 0.114; ZnSO<sub>4</sub>, 0.0882; MnCl<sub>2</sub>·4H<sub>2</sub>O, 0.014; MoO<sub>3</sub>, 0.007; CuSO<sub>4</sub>·5H<sub>2</sub>O, 0.015; Co (NO<sub>3</sub>)<sub>6</sub>·H<sub>2</sub>O, 0.0048. Then, the strain was cultured in Erlenmeyer glass flask containing 1L modified BBM media. The Carbon source was provided by continuous aeration and bubbling sterile air. The culture was incubated at 30 °C ± 1 °C under light intensity of 50 µmol photon s<sup>-1</sup>m<sup>-2</sup> using fluorescent lamps and provided with the photoperiod of 12 h light: 12 h dark cycle for 24 days.

### 2.3. Morphological and molecular identification of microalgal strain

Morphological examination was carried out with the aid of light microscope (MCX100-micros Austria). Modified Cetyl trimethylammonium bromide (CTAB) method was used to separate genomic DNA from algal cells. 0.25 g of harvested algal cells was grounded and dissolved in pre-heated (65 °C) 1.5 ml of CTAB buffer. Sample was subjected to mechanical degradation (Vortex) by using 3 mm sterile glass. After that, samples were digested enzymatically by adding 5 µl of Proteinase K, 30 µl of 10% SDS and 10 µl lysozyme and incubated at 37 °C for 1 h. For separation and purification of DNA, 100 ml of CTAB and 80 µl of 5 M NaCl

was added and incubated again at 65 °C for 15 mins in water bath. For separation of proteins from genomic DNA, 500 µl of Phenol: Chloroform: Isoamyl alcohol (PCI) was added and centrifuged at 10,000 rpm for 20 mins, which resulted in separation of liquid and organic phase. The liquid phase was separated in a new eppendorf tube and washed twice with PCI. Then, 500 µl of isopropanol (chilled) and 300 µl of 3 M sodium acetate solutions was added and incubated at 4 °C for over night to get precipitation. Precipitates were pelleted out by centrifugation at 10,000 rpm and –4°C temperature next day and washed with 200 µl of 70% ethanol solution to remove any impurity. Finally, the palette was dissolved in 50 µl of TE buffer for further use in Standard Gel electrophoresis and DNA sequencing. DNA sequencing has been carried out from MACROGEN (South Korea) public biotechnology company. Further, BLASTn algorithm and MUSCLE alignment tool were used to search for sequence homology of obtained sequences, against sequences in nucleotide database of National Center for Biotechnology Information (NCBI) (Rismani-Yazdi et al., 2011). DNA sequence Genbank ID for isolated microalgae strain (MT 858355.1) was obtained from NCBI. MEGA (version 7) software was used to analyze maximum likelihood and distance between species, based on phylogenetic tree construction (Chaidir et al., 2016).

#### 2.4. Experimental design for optimization and statistical analysis

In order to optimize growth characteristics, central composite Design (CCD) of experiment was used where pH and phosphate concentration was considered as independent variables. Design has two-factor levels and five central points repetitions. Factor levels of –1 and +1 were assigned to lowest and highest parametric values by retaining alpha value ( $\alpha$ ) at 1 (Table 1). The design of experiment has been resulted in 13 treatments including five control levels (Table 2). The significance of linear, square and two-way variable interaction (pH and phosphate concentration) on responses (specific growth rate and biomass productivity) has been estimated using ANOVA, Pareto charts and factorial plots with the significance of ( $p < 0.05$ ) at 95% confidence level. Response surface, regression analysis, Analysis of variance (ANOVA), 2D Counter, 3D Surface and factorial plot for variable interactions and response values were carried out using Minitab (version 18), to assess the significance of modal variables and response maximization up on optimization of operational parameters.

#### 2.5. Growth characteristics

Measuring microalgal cell dry weight at early and late exponential phase of cultivation, day 3 and 21, respectively, assessed specific growth rate and biomass productivity. For that, 100 ml of sample cell cultures was centrifuged at 4000 rpm (12 mins) and cellular pallets were oven dried after washing twice with distilled water. The specific growth rate ( $g L^{-1} d^{-1}$ ) was determined using following formula;

$$\mu = \ln(Z_t - Z_0) / (t_f - t_0) \quad (1)$$

Where  $\mu$  ( $g d^{-1} L^{-1}$ ) is a specific growth rate,  $Z_0$  and  $Z_t$  are number of cells at  $t_0$  and  $t_f$  respectively.

**Table 1**

Central composite Design of experiment for optimization of Parameters for specific growth rate and biomass productivity.

Experimental variables	Symbols	Factor levels	
		–1	+1
Phosphate conc. (g / L)	A	0.023	0.115
pH	B	6	9

The biomass productivity ( $g d^{-1} L^{-1}$ ) was estimated at exponential growth phase by using equation where  $Z_2$  and  $Z_1$  are dry cellular biomass ( $g L^{-1}$ ) taken at final and initial time, respectively by using equation (2).

$$\text{Biomass productivity} = (Z_2 - Z_1) / (t_2 - t_1) \quad (2)$$

Generation time, T, expressed in units of time was calculated from estimation of  $\mu$  by using equation (3);

$$T = \ln 2 / \mu \quad (3)$$

The total carbohydrates content of 21 days aged cellular cultures was estimated using protocol of modified phenol-sulfuric acid method, by following acidic pretreatment and taking glucose as standard (Dubois et al., 1956).

#### 2.6. Biomass analysis

For FT-IR analysis, 10 ml of cells suspension from each treatment were pelleted out at 5000 rpm (10 mins). Cell pallets were washed two fold using distill water and desiccated for 35 mins. The analysis was carried out in FTIR spectrometer (Perkin-Elmer Tensor 27, Bruker) fitted out with ZnSe ATR detector with the resolution of 1 cm and 15 scans, in range of 4000–600  $cm^{-1}$ . The quantity of carbohydrates, lipids and proteins were assessed and compared by determining the absorbance intensity of spectral peaks assigned to each biomolecule. (SEM, Vega3 TESCAN) coupled with energy dispersive X-ray spectroscopy system (EDS, Bruker) was used to assess elemental composition and surface analysis of optimized biomass.

#### 2.7. Saccharification and submerged fermentation (SmF)

Saccharification was carried out by acid catalyzed hydrolysis of biomass. 500 mg of oven dried and finely ground biomass was subjected to 2%  $H_2SO_4$  solution and autoclaved at 121 °C for 15mins (Hossain et al., 2015). The hydrolysate was left for 48 h with continuous agitation at 200 rpm and 45 °C for further catalysis of carbohydrates to fermentable sugars. Yeast (*Saccharomyces cerevisiae*) based submerged fermentation was carried out for bioethanol production. Yeast extract peptone dextrose (YDP) medium was used to activate yeast cells. Cultures were taken from logarithmic phase and centrifuged at 9000 rpm for 10mins. Pelleted cells were transferred to hydrolyzed sugars solution provided with constant shanking for 5 days at 800 rpm (30 °C) (Faizal et al., 2021; Selvan et al., 2019).

#### 2.8. Estimation and characterization of bioethanol

Solvent extraction and dichromate oxidation method was utilized to measure concentration of bioethanol. For that, 15 g of  $K_2Cr_2O_7$  were dissolved in 100 ml of 5 M  $H_2SO_4$  solution. Tri-n-butyl phosphate (TBP) was used as bioethanol extractant. Standard ethanol solutions (0%–30%) or sample were mixed with TBP in 1:1 in 2 ml eppendorf tubes and vortexed vigorously until two phases separated out. 500 µl of upper phase solution shifted to fresh tube and mixed with uniform amount of dichromate reagent. Solution were again vortexed until phases separates out. Then, lower phase was taken and diluted up to 10 times with standard solutions and sample (Miah et al., 2017). Optical densities of solution were measured at 595 nm ( $OD_{595}$ ) in UV-spectrophotometer (SPECORD 200 plus, analytikjena Germany). Unknown bioethanol concentration in sample was estimated from ethanol stander curve.

**Table 2**  
Central composite design of Experiment and Response values.

Run Order	Phosphate. Conc. (g / L)	PH	Specific growth rate (day <sup>-1</sup> )		Biomass productivity (g L <sup>-1</sup> day <sup>-1</sup> )	
			Experimental	Predicted	Experimental	Predicted
1	0.115	6	0.327	0.327	0.324	0.333
2	0.115	9	0.342	0.342	0.497	0.494
3	0.115	7.5	0.332	0.332	0.421	0.415
4	0.069	7.5	0.33	0.328	0.361	0.350
5	0.023	9	0.293	0.291	0.257	0.244
6	0.069	6	0.325	0.327	0.293	0.285
7	0.069	7.5	0.328	0.328	0.349	0.350
8	0.069	7.5	0.327	0.328	0.357	0.350
9	0.023	6	0.295	0.293	0.146	0.145
10	0.069	9	0.331	0.333	0.398	0.414
11	0.069	7.5	0.33	0.328	0.34	0.350
12	0.023	7.5	0.287	0.290	0.181	0.195
13	0.069	7.5	0.326	0.328	0.353	0.350

### 3. Results

#### 3.1. Strain isolation and identification

The algal sample collected from fresh water was isolated, purified and examined under light microscope (100X lens with oil emulsion). The morphological examination of algal isolate revealed unicellular, narrow and pointed like a needle shaped configuration (Fig. 1), resembling member of fresh water algal family: *Chlorellaceae*, genus: *Closteriopsis* and specie: *acicularis* (John et al., n.d.). Further, morphological identification was carried out to confirm taxonomic and phylogenetic relationship of isolate (MA1). 18S rRNA gene was used as nuclear marker for sequencing of Genomic DNA. This gene is conserve and moderate in evolution process, which makes it suitable for molecular identification of algae (Chen et al., 2017; Tang et al., 2012). Gene sequence of isolate was BLASTn in National Center for Biotechnology Information (NCBI) database, which disclosed high similarity of isolate (MA1) with other strains in database. To determine evolutionary relationship, a phylogenetic tree of maximum likelihood was constructed using MEGA software version 7 (Chaidir et al., 2016) along with MUSCLE alignment tool (Rismani-Yazdi et al., 2011) (Fig. 2). The evolutionary lineage of species and organisms are represented by phylogenetic tree that relates one with their own distinct ancestor (Yanuhar et al., 2019). The phylogeny tree constructed with 12 closely related species of microalgae based on information inferred from NCBI Genbank, which suggested that the isolate sequence

was clustered with 3 microalgae specie (Fig. 2), namely *Closteriopsis acicularis* strain (Genbank ID: HM066009.1, MF086580.1 and FM205847.1) with 96.28%, 95.39% and 96.30% sequence similarities, respectively.

#### 3.2. Statistical analysis and optimization of phosphate-concentration and pH

Present study was conducted to exhibit the effect of phosphate concentration and pH on growth characteristics of indigenous microalgae *Closteriopsis acicularis*. The second order polynomial model was formulated for experimental response values of linear, square and interaction terms, by using multiple regression analysis and Minitab (software version 18). Central composite Design (CCD) of experiment has been used to compose treatments for independent variables at two factors level (low (-1), high (+1)) by retaining alpha value at 1 (Table 1).

For all 13 treatments, it was observed a constant growth trend of *Closteriopsis acicularis* with short lag phase of 2 days and long exponential growth phase till day 21th of cultivation. The response values of specific growth rate (day<sup>-1</sup>) and biomass productivity (g L<sup>-1</sup> day<sup>-1</sup>) of cultures taken from late exponential growth phase, was correlated with two independent variables (phosphate concentration and pH) by using predictive regression model equation in coded units, in the form of regression equations (4) and (5) respectively.

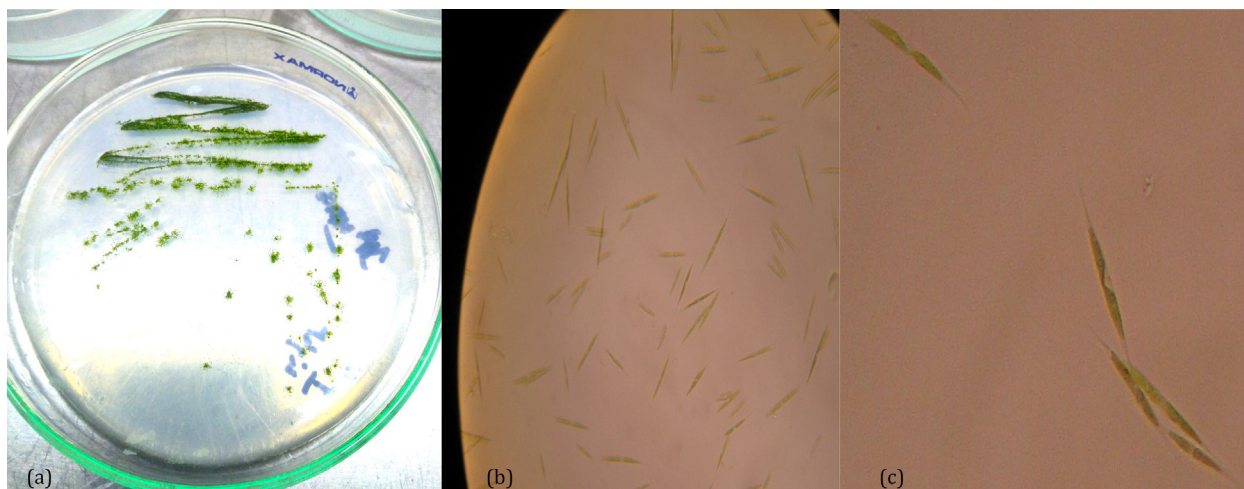


**Fig. 1.** Isolation of fresh water green microalgae *Closteriopsis acicularis* (a) streak plate technique, (b, c) light microscopic images at 100X.

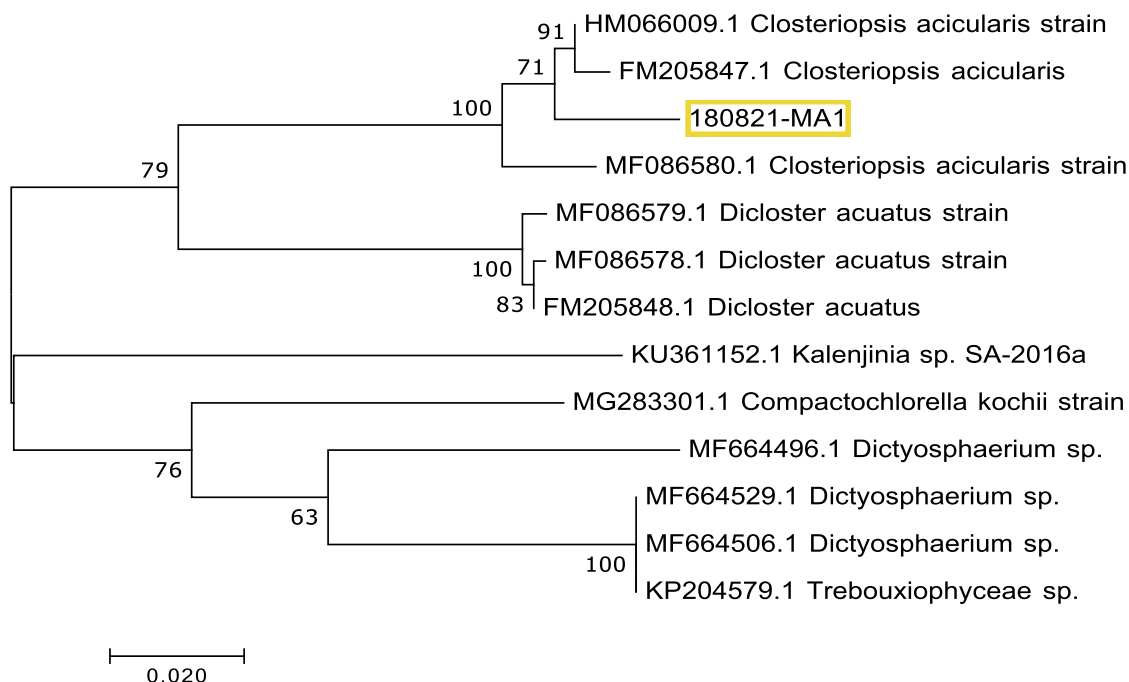


Fig. 2. The phylogenetic tree of fresh water green microalgae isolate *Closteriopsis acicularis* (MA1).

$$\text{Specific Growth rate} = 0.3301 + 1.058A - 0.01674B - 7.708A.A + 0.000973B.B + 0.0616A.B \quad (4)$$

$$\text{Biomass productivity} = -0.148 + 3.663A + 0.0340B - 21.48A.A - 0.00042B.B + 0.2246A.B \quad (5)$$

The results of Predictive regression model shows that phosphate-conc. and pH strongly affected the output responses (Table 2). The maximum specific growth rate ( $\text{day}^{-1}$ ) in this study was determined as  $0.342 \text{ day}^{-1}$ , generation time of 48.72 hrs in treatment 2 when phosphate concentration of  $0.115 \text{ g L}^{-1}$  and pH 9 was used as cultivation conditions (Table 2). The maximum biomass productivity was obtained  $0.497 \text{ g L}^{-1} \text{ day}^{-1}$  with  $0.115 \text{ g/L}$  phosphate-concentration and pH 9 measured at late exponential phase of growth.

The prediction capability of model was evaluated by Coefficients of determination  $R^2$  which shows the correlation between predicted and experimental response values of growth characteris-

tics. The high  $R^2$  and near adj.  $R^2$  values of responses implies the accurate prediction of statistical model (Tables 3 and 4).

Factorial plots for main effect of phosphate concentration and pH on specific growth rate and biomass productivity have shown greater influential effect of phosphate concentration on both responses, where as pH has shown more influential effect on biomass productivity (Fig. 3a and c). It is observed clearly that the interaction effect of phosphate concentration and pH was optimum at  $0.1 \text{ g L}^{-1}$  and 9, respectively, for specific growth rate (Fig. 3b), where as the interaction effect on biomass productivity was optimum at pH 9 and phosphate concentration  $> 0.1 \text{ g L}^{-1}$ .

Pareto Charts of Standardized effect with 95% confidence level was plotted to determine the significant effect of variables on their linear (A = phosphate concentration and B = pH), square ( $A^2$  and  $B^2$ ) and interaction terms (AB) of specific growth rate and biomass productivity. The well-noted vertical line indicates the statistically significant threshold (average value 2.36) for responses (Fig. 4). It is clear from Pareto chart that individual linear variables, squares and their interactions are significantly associated with responses except for the square term of pH (BB), which revealed insignificant association with both responses (Fig. 4a and b).

Table 3  
Statistical analysis (ANOVA) of CCD for Specific growth rate ( $\text{day}^{-1}$ ).

Source	DF	Adj SS	Adj MS	F-Value	P-Value
Model	5	0.003565	0.000713	136.64	0
Linear	2	0.002706	0.001353	259.27	0
Phosphate. Conc.	1	0.002646	0.002646	507.01	0
pH	1	0.00006	0.00006	11.53	0.012
Square	2	0.000787	0.000394	75.41	0
Phosphate. conc.*Phosphate. Conc.	1	0.000735	0.000735	140.79	0
pH*pH	1	0.000013	0.000013	2.54	0.155
2-Way Interaction	1	0.000072	0.000072	13.84	0.007
Phosphate. Conc.*pH	1	0.000072	0.000072	13.84	0.007
Error	7	0.000037	0.000005		
Lack-of-Fit	3	0.000024	0.000008	2.47	0.201
Pure Error	4	0.000013	0.000003		
Total	12	0.003602			

$R^2 = 98.99\%$ ,  $R^2$  (adj.) =  $98.26\%$ ,  $R^2$  (pred.) =  $94.35\%$

**Table 4**  
Statistical analysis (ANOVA) of CCD for Biomass Productivity ( $\text{g L}^{-1} \text{day}^{-1}$ ).

Source	DF	Adj SS	Adj MS	F-Value	P-Value
Model	5	0.105124	0.021025	130.49	0
Linear	2	0.097381	0.04869	302.19	0
Phosphate. conc.	1	0.072161	0.072161	447.86	0
pH	1	0.02522	0.02522	156.53	0
Square	2	0.006782	0.003391	21.05	0.001
Phosphate. conc.*Phosphate. conc.	1	0.005705	0.005705	35.41	0.001
pH*pH	1	0.000002	0.000002	0.02	0.905
2-Way Interaction	1	0.000961	0.000961	5.96	0.045
Phosphate. conc.*pH	1	0.000961	0.000961	5.96	0.045
Error	7	0.001128	0.000161		
Lack-of-Fit	3	0.000868	0.000289	4.45	0.092
Pure Error	4	0.00026	0.000065		
Total	12	0.106252			

$R^2 = 98.94\%$ ,  $R^2(\text{adj.}) = 98.18\%$ ,  $R^2(\text{pred.}) = 91.62\%$

In order to take further insight, Analysis of variance (ANOVA) was performed for F-statistics (F-value) and Probability (P-value).

Higher F-value and lower P-value ( $P < 0.05$ ) are generally used as an indicator of modal variable and their interaction terms as statis-

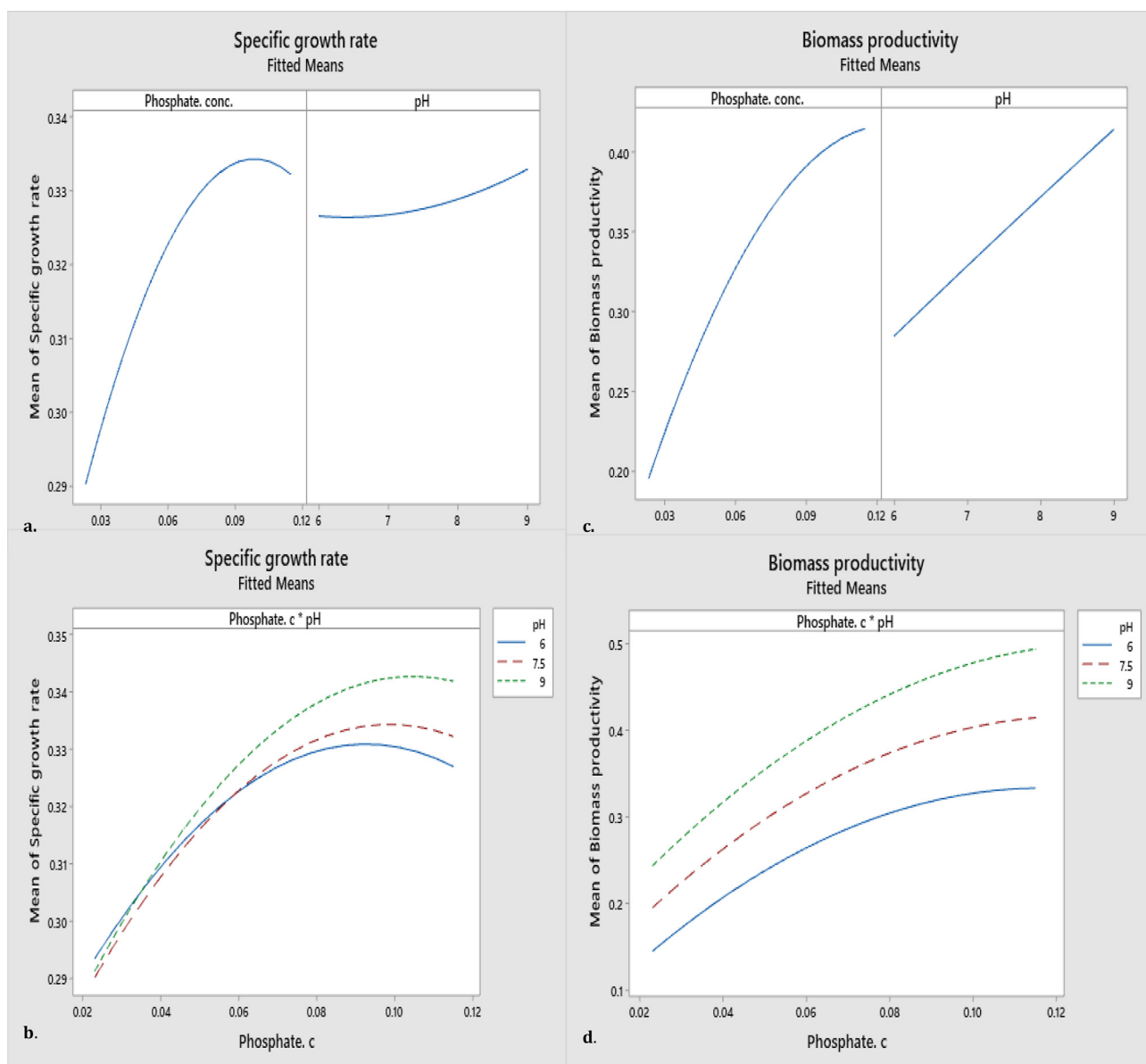


**Fig. 3.** Factorial plots for main effect (a), interaction effect (b) of specific growth rate and for main effect (c), interaction effect (d) of biomass productivity of *Closteriopsis acicularis*.

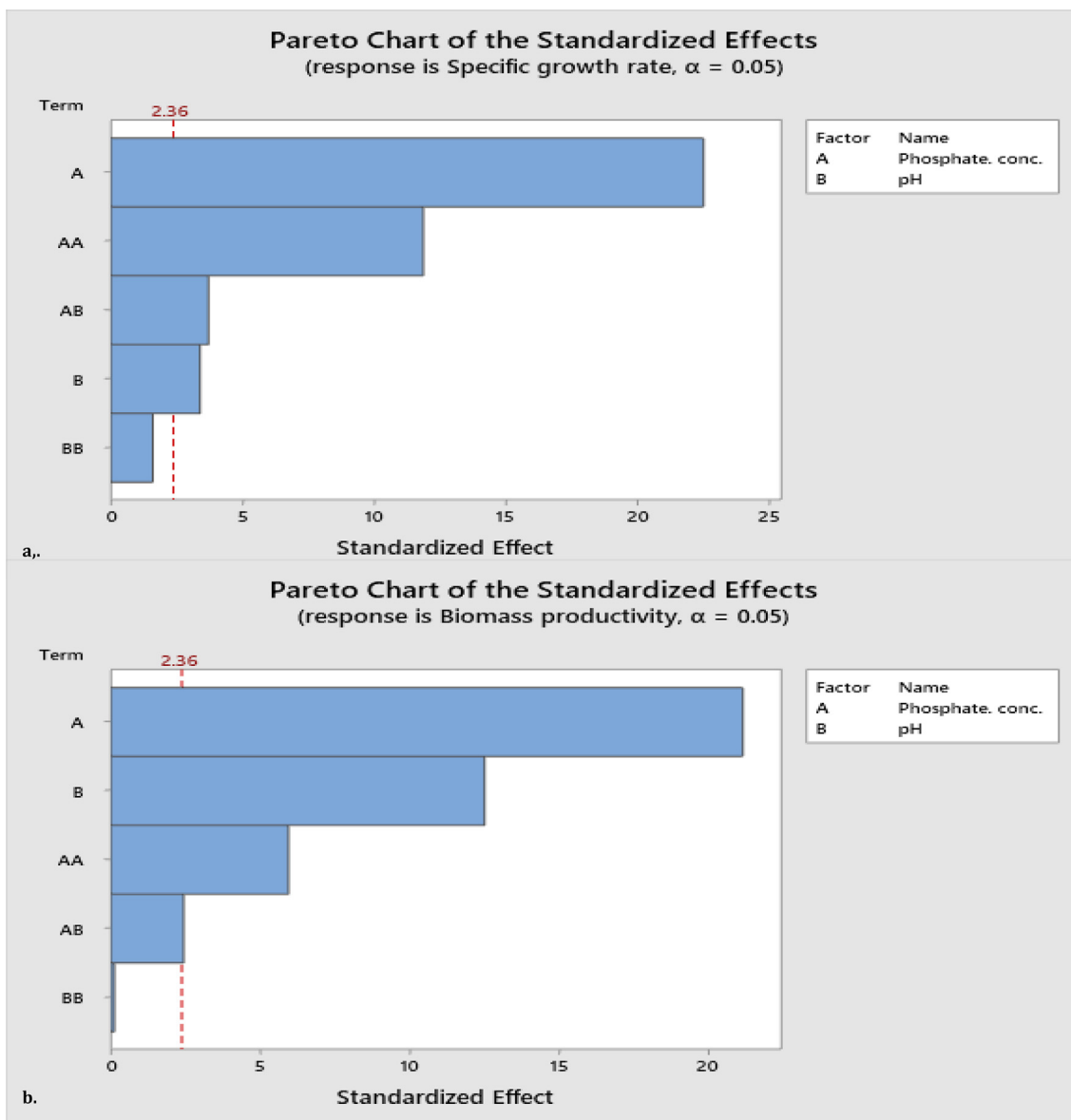


**Fig. 4.** Standardized Pareto chart showing statistical results for screening of two variables involved in optimization of *Closteriopsis acicularis* for; (a) Specific growth rate, (b) Biomass productivity. The statistical design was CCD with one replication and five center points. Statistically significant threshold is 2.36.

tically significant or insignificant (Naghypour et al., 2016; Sultana et al., 2020). Tables 3 and 4 shows ANOVA for response values of specific growth rate and biomass productivity, respectively. The model P-values for both responses are extremely low ( $P = 0.000$ ), which indicates response associated significance of predictive model. The linear terms of all variables have shown high significance at 95% confidence level ( $P < 0.05$ ,  $\alpha = 0.05$ ). The square terms for pH ( $B^2$ ) for both responses were insignificant, whereas interaction term for both responses was significant. The overall statistical analysis of variance results was in accordance with CCD Pareto charts data.

### 3.3. Response surface analysis

The response Surface method (RSM) has been used to determine interaction of phosphate-concentration and pH for optimum responses, by fixing the two variables between  $-1$  and  $+1$  factor levels. The 2D-counter plots and 3D-surface plots for biomass and lipids production (mg / L) are shown in Fig. 5. Fig. 5a and 5b

shows the optimum variable range for high specific growth rate of *Closteriopsis acicularis*. It is clear from Fig. 5a that specific growth rate enhanced with higher phosphate-concentration and pH. The maximum growth rate was achieved with phosphate-concentration at  $+1$  level (0.115 g/L) and pH at  $+1$  level (9). The highest response value for specific growth rate ( $>0.336$  g day $^{-1}$ ) was achieved with coupled effect of high pH and phosphate-concentration as shown in counter and surface plot of specific growth rate (Fig. 5a and b).

The biomass productivity has been observed maximum ( $>0.45$  g L $^{-1}$  day $^{-1}$ ) with pH and phosphate-concentration at  $+1$  levels (Fig. 5c and d).

### 3.4. Characterization of biomass by FTIR and SEM-EDS

In order to analyze the effect of optimized cultivation conditions for enhanced bimolecular accumulation of *Closteriopsis acicularis*, the biomass of four treatments (2, 3, 4 and 10) which yielded

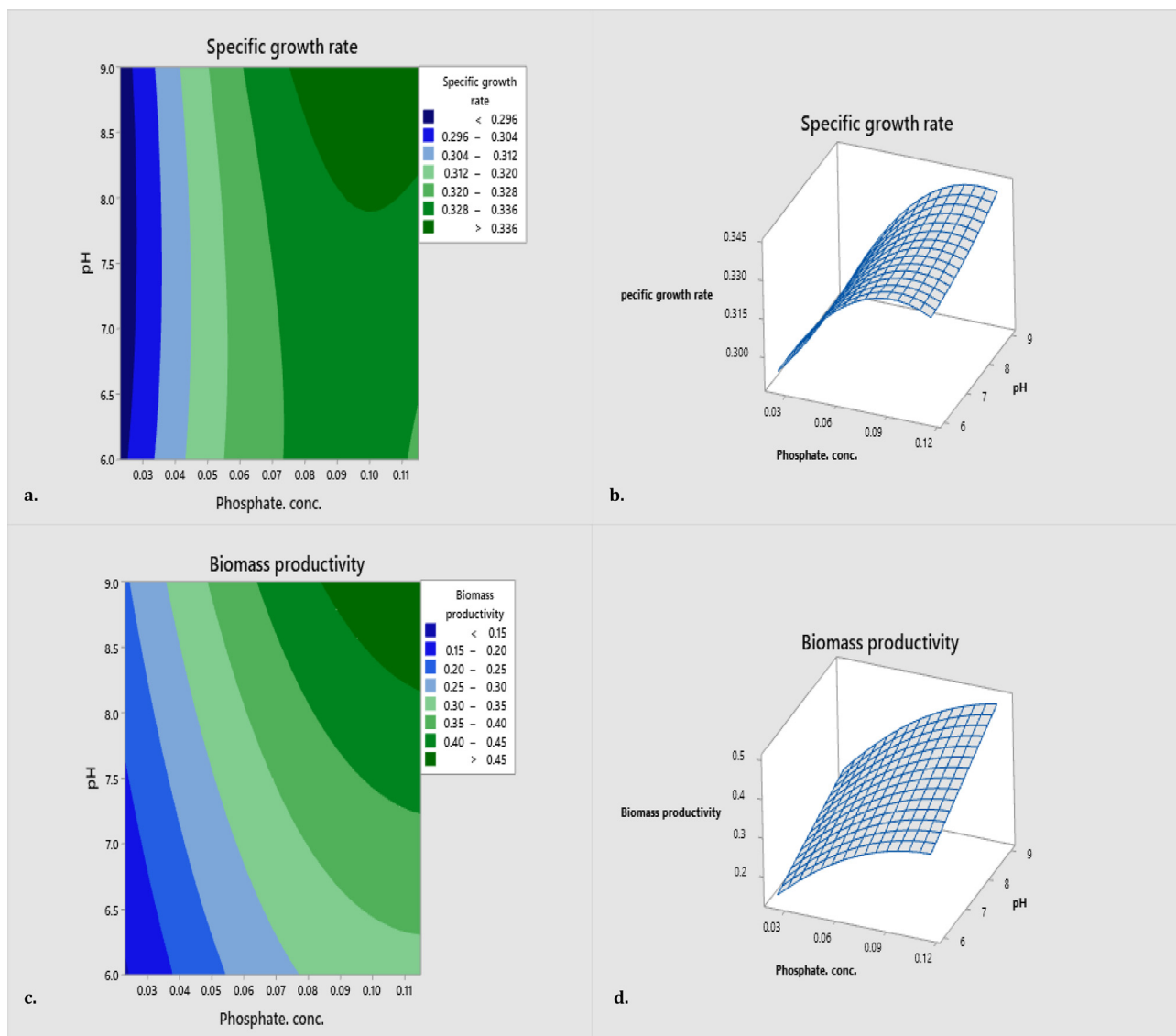


Fig. 5. RSM (2D-counter, 3D-surface plots of two way interaction of variables) for estimated specific growth rates (a, b) and biomass productivity (c,d) of *Closteriopsis acicularis* as a function of phosphate conc. and pH.

considerably high biomass productivity has been characterized by using FT-IR.

The FTIR spectra visualized the outcome of optimum conditions on biochemical composition of these biomasses. Typically, absorption peaks of FTIR spectra for biochemical characterization of proteins, lipids and carbohydrates provides useful information in range of 600–4000  $\text{cm}^{-1}$ . For microalgae biomass, typically the spectral bands in range of 900–1200  $\text{cm}^{-1}$ , 1540–1640  $\text{cm}^{-1}$  and 1735–2917  $\text{cm}^{-1}$  are assigned to functional groups of carbohydrates, proteins and lipids respectively (Piasecka et al., 2020).

The FTIR spectra of biomass grown in treatment 2, 3, 4 and 10 (Table 2) have been shown in Fig. 6d, 6a, 6b and 6c, respectively. Beer-lambert’s law describes the direct relation of the absorbance of light to the concentration of compound and path length (Huesemann et al., 2016; Lee, 1999). The absorbance value and spectral peaks intensity was compared for determining extent of biomolecules accumulation in all four biomasses (Fig. 6e).

The biomass grown at high phosphate concentration and high pH (treatment 2) have shown maximum absorption and intensity

of spectral peaks for stretching of  $\text{—C—O—C—}$  group of carbohydrates at 1059.67  $\text{cm}^{-1}$  (Giordano et al., 2001), amide I and amide II functional groups of proteins at 1627.64 (Movasaghi et al., 2008; Naumann et al., 2009) and 1537.58  $\text{cm}^{-1}$  (Coates, 2006; Stehfest et al., 2005) respectively, where as asymmetric and symmetric stretching of  $\text{—CH}_2$  group of saturated fatty acids at 2920.16 (Naumann et al., 2009) and 2851.44  $\text{cm}^{-1}$  (Giordano et al., 2001) respectively. It is also observed clearly from Fig. 6e, that all biomasses have shown almost same biochemical composition in terms of spectral assignments in characteristic regions of functional groups assigned to each compound, however with different maximum absorption and spectral peaks intensity.

The elemental make-up of microalgae biomass from two unlike treatments (2 and 4, Table 2) was compared to with each other to find out the impact of phosphate concentration and pH on accumulation of organic and inorganic elements. The biomass grown in medium with high phosphate concentration and pH (0.115  $\text{g L}^{-1}$ , 9) has shown high accumulation of carbon, phosphorus, oxygen and inorganic elements except sulphur and nitrogen (Fig. 7).



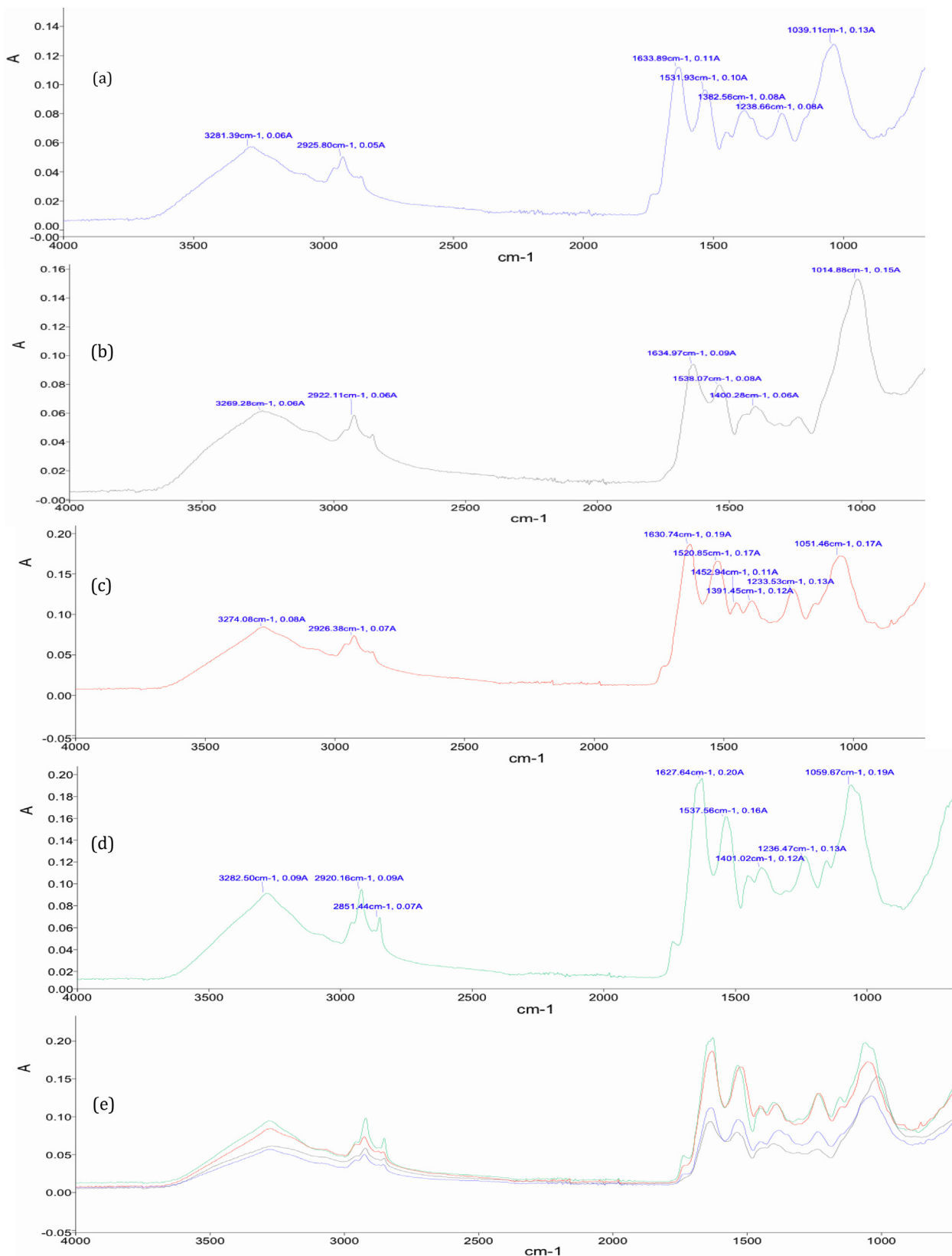


**Fig. 6.** FT-IR spectra of *Closteriopsis acicularis* biomass grown autotrophically, (a) biomass of treatment 3, (b) biomass of treatment 4, (c) biomass of treatment 10, (d) biomass of treatment 2, (e) comparative spectra of optimized and un-Optimized biomass, in the range of 600–4000  $\text{cm}^{-1}$ .

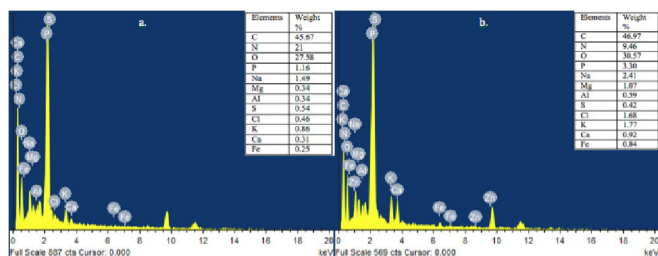


Fig. 7. SEM-EDS spectra of microalgae *Closteriopsis acicularis* biomass in: (a) low phosphate conc. and pH, (b) high phosphate conc. and pH.

### 3.5. Bioethanol production and estimation

In this study, the carbohydrates content of *Closteriopsis acicularis* biomass was estimated as 58% (w/w) of CDW. After the acid catalyzed saccharification of biomass, the monosaccharide's (glucose) concentration was estimated as 29.3 g/L of biomass. Nearly all the glucose was consumed after 12hrs of incubation with maximum of 14.9 g/L of ethanol production. The ethanol yield was measured as 51 % g ethanol/g glucose, in fermentation process.

## 4. Discussion

The synthetic metabolism of microalgae for rapid rate of growth, excessive biomass and biomolecules accumulation, could be improved with the change in certain cultivation conditions such as temperature, pH, nutrient concentration, light, CO<sub>2</sub> level and salinity. To date numerous studies have been reported that illustrates the individual as well as combined effect of different parameters for production of microalgae biomass (Miranda et al., 2016; Peng et al., 2020; Yaakob et al., 2021; F. Yang et al., 2014). Faster growth rate and high biomass productivity are significant key feature of microalgal species for use in commercial purposes, as it favors robust growth over microorganism contamination in large scale outdoor facilities for cultivation of microalgae (Tan & Lee, 2016). Our results shows that the metabolic reactions of microalgae used in present study (*Closteriopsis acicularis*) were strongly affected by varying concentration of phosphate and pH. High phosphate concentration coupled with high pH has resulted in significantly rapid growth rate and biomass productivity. Growth rate and phosphate concentration are directly correlated to biomass productivity of microalgae (Yaakob et al., 2021).

The maximum specific growth rate (0.342 day<sup>-1</sup>) and higher biomass productivity (0.497 g L<sup>-1</sup> day<sup>-1</sup>) were obtained in treatment with high levels of phosphate concentration and pH. The maximum specific growth rate obtained in this study was comparable with specific growth rate of microalgae reported earlier such as *Chlorella* sp. BA-167 (0.39 ± 0.01), *Monoraphidium* sp. BA-165 (0.35 ± 0.01) day<sup>-1</sup> (Klin et al., 2020). Biomass productivity obtained was found greater than biomass productivity of *Chlorella vulgaris* (75.57 ± 1.93 mg L<sup>-1</sup> day<sup>-1</sup>) (Fozer et al., 2019), *Parachlorella kessleri* (88 mg L<sup>-1</sup> day<sup>-1</sup>) (Fields et al., 2021), *Chlorella sorokiniana* (146.07 mg L<sup>-1</sup> day<sup>-1</sup>) (Guldhe et al., 2019) outlined in earlier studies. Our findings are consistent with literature reported earlier that high phosphate concentration resulted in high growth rate and biomass yield, where the optimum phosphate concentration of microalgae ranges in 0.001 g L<sup>-1</sup> to 0.179 g L<sup>-1</sup> (Roopnarain et al., 2014). According to literature reported, microalgae cultures grown at pH 8 to 9 favors high growth and biomass productivity and pH > 9 limits availability of CO<sub>2</sub> and HCO<sub>3</sub><sup>-1</sup> that are essential for algal growth (Bartley et al., 2016; Difusa et al., 2015; Qiu et al., 2017). Studies also revealed that microalgae favors gradual rise of pH and pH 8.2 favors rapid nitrogen assimilation and conversion of nitrates to ammonia, which results in high alkalinity

at later stage of exponential phase (Difusa et al., 2015; Moreno-Garcia et al., 2019). Phosphorus is a requisite nutrient for growth and cell division of algae. Microalgae has high tendency to absorb phosphorus from medium and level of phosphorus uptake is linearly proportional to biomass production (Fu et al., 2017; Yaakob et al., 2021).

The characteristics of microalgae growth are directly affected by varying concentration of phosphate and pH (Z. Yang et al., 2018; Lovio-Fragoso et al., 2019; Corredor et al., 2021). High concentration of elements tends to increase cell size and surface to volume ratio, which in turn favors high concentration of chloroplast and photosynthetic efficiency (Klin et al., 2018). Characterization of optimized biomass shows high carbon, oxygen and phosphorus accumulation with resulted maximum absorption peaks in spectral region of carbohydrates and lipids. The carbohydrates content (58% (w/w) of CDW) of optimized biomass was found comparably higher than carbohydrates content of strains reported earlier such as *Ulva fasciata* (46.96%), *Chlorella salina* (50%) (Barakat et al., 2021; Mayers et al., 2018) and comparable with the highest carbohydrate content of 49% and 50% reported for commercially important microalgae *Chlamydomonas* sp. (Morales-Sánchez et al., 2020) and *Chlorella vulgaris* (Ferreira et al., 2019) respectively. The high carbohydrate content is favorable for providing the amount of fermentable sugars for ethanol production. It was observed decrease in nitrogen and sulfur accumulation in elemental make up of optimized biomass which agrees well with the results of infrared spectroscopy of optimized biomass that shows very few absorptions in spectral region of proteins. The results of present study indicates metabolic shift in synthetic mechanisms of biomolecules that resulted in increase in carbohydrates and lipids accumulation in phosphorous rich medium coupled with high pH and associated less protein formation. Several studies have shown the phosphate concentration and pH related impact on metabolic shifts towards accumulation of more carbohydrates and lipids in microalgae (Difusa et al., 2015; Roopnarain et al., 2014). The ethanol yield (51 % g ethanol/g glucose) obtained after fermentation of sugars was found comparable with ethanol yields attained in studies reported earlier (Kim et al., 2020; Adela & Loh 2015).

## 5. Conclusion

The Response surface method CCD was utilized to optimize phosphate-concentration and pH for higher specific growth rate and biomass productivity of indigenous microalgae *Closteriopsis acicularis* strain isolated from local fresh water body, Islamabad Pakistan. The isolate responded effectively at high phosphate-concentration (0.115 g/L) and high pH (9), for accumulation of biomass with considerably less generation time. It is observed in FTIR analysis that optimized biomass has accumulated more biomolecules in terms of carbohydrates, in comparison to un-optimized biomass. Additionally, it is concluded that the elemental composition of optimized biomass has more %weight of most macro and micronutrients (C, O, P, Na, Mg, Al, K, Ca and Fe) except nitrogen and sulphur, which are main constituents of proteins.

Our findings of Saccharification and fermentation of optimized biomass concluded that *Closteriopsis acicularis* could be potential candidate for bioethanol production due to high carbohydrate content (58%) and fermentable sugar 29.3 g L<sup>-1</sup> of biomass. However, there is further screening and strategic optimization of fermentation parameters required to improve the maximum ethanol production, which is observed 14.9 g/L in this study.

### CRedit authorship contribution statement

**Farhana Bibi:** Data curation, Formal analysis, Methodology, Writing – original draft. **Humaira Yasmin:** Analysis, Conceptualiza-

tion, Review and editing. **Asif Jamal:** Analysis, Conceptualization, Review and editing. **Mohammad S. AL-Harbie:** Resource funding, Review. **Mushtaq Ahmad:** Formal analysis, Review and editing. **Zafar Mehmood:** Data analysis, Review and editing. **Bashir Ahmad:** Analysis, Review and editing. **Bassem N. Samra:** Analysis, Conceptualization, Review and editing. **Atef F. Ahmed:** Analysis, Conceptualization, Review and editing. **Muhammad Ishtiaq Ali:** Review and editing, Conceptualization, Supervision, Methodology, Project administration.

### Declaration of Competing Interest

The authors declare that they have no known competing financial interests or personal relationships that could have appeared to influence the work reported in this paper.

### Acknowledgments

We acknowledge Pakistan Science Foundation for funding under project title PSF/NSLP/C-QAU895. The authors would also extend their sincere appreciation to the Taif University Researchers Supporting Project number (TURSP-2020/64), Taif University, Taif, Saudi Arabia.

### Ethics approval

Not Applicable.

### Consent to participate

All authors consent to participate in this manuscript.

### Consent for publication

All authors consent to publish this manuscript in the Saudi Journal of Biological Science.

### Availability of data and material

Data will be available on request to the corresponding or first author.

### Code availability

Not Applicable.

### References

- Adela, B.N., Loh, S.K., 2015. Optimisation of fermentation conditions for bioethanol production from oil palm trunk sap by *Saccharomyces cerevisiae*. *Malaysian J. Microbiol.* <https://doi.org/10.21161/mjm.12814>.
- Almutairi, A.W., El-Sayed, A.E.K.B., Reda, M.M., 2020. Combined effect of salinity and pH on lipid content and fatty acid composition of *Tisochrysis lutea*. *Saudi J. Biol. Sci.* 27 (12), 3553–3558. <https://doi.org/10.1016/j.sjbs.2020.07.027>.
- Almutairi, A.W., El-Sayed, A.E.K.B., Reda, M.M., 2021. Evaluation of high salinity adaptation for lipid bio-accumulation in the green microalga *Chlorella vulgaris*. *Saudi J. Biol. Sci.* 28 (7), 3981–3988. <https://doi.org/10.1016/j.sjbs.2021.04.007>.
- Ameen, F., AlNadhari, S., Al-Homaidan, A.A., 2021. Marine microorganisms as an untapped source of bioactive compounds. *Saudi J. Biol. Sci.* 28 (1), 224–231. <https://doi.org/10.1016/j.sjbs.2020.09.052>.
- Barakat, K.M., El-Sayed, H.S., Khairy, H.M., El-Sheikh, M.A., Al-Rashed, S.A., Arif, I.A., Elshobary, M.E., 2021. Effects of ocean acidification on the growth and biochemical composition of a green alga (*Ulva fasciata*) and its associated microbiota. *Saudi J. Biol. Sci.* 28 (9), 5106–5114. <https://doi.org/10.1016/j.sjbs.2021.05.029>.
- Bartley, M.L., Boeing, W.J., Daniel, D., Dungan, B.N., Schaub, T., 2016. Optimization of environmental parameters for *Nannochloropsis salina* growth and lipid content using the response surface method and invading organisms. *J. Appl. Phycol.* 28 (1), 15–24. <https://doi.org/10.1007/s10811-015-0567-8>.
- Bušić, A., Mardetko, N., Kundas, S., Morzak, G., Belskaya, H., Ivančić Šantek, M., Komes, D., Novak, S., Šantek, B., 2018. Bioethanol Production from Renewable Raw Materials and Its Separation and Purification: A Review. *Food Technol. Biotechnol.* 56 (3). <https://doi.org/10.17113/ftb.56.03.18.5546>.
- Chaidir, Z., Fadrija, N., Armaini, Zainul, R., 2016. Isolation and molecular identification of freshwater microalgae in Maninjau Lake West Sumatra. In: *Der Pharmacia Lettre*, vol. 8, Issue 20, pp. 177–187. [10.31227/osf.io/nbcuf](https://doi.org/10.31227/osf.io/nbcuf).
- Chakraborty, R., Mukhopadhyay, P., 2020. Green Fuel Blending: A Pollution Reduction Approach. In: Hashmi, S., Choudhury, I.A. (Eds.), *Encyclopedia of Renewable and Sustainable Materials*. Elsevier, pp. 487–500. [10.1016/B978-0-12-803581-8.11019-7](https://doi.org/10.1016/B978-0-12-803581-8.11019-7).
- Chen, C.Y., Durbin, E.G., 1994. Effects of pH on the growth and carbon uptake of marine phytoplankton. *Mar. Ecol. Prog. Ser.* 109 (1), 83–94. <https://doi.org/10.3354/meps109083>.
- Chen, Y., Li, X.-yang, Sun, Z., Zhou, Z.-gang, 2017. Isolation and identification of *Choricystis minor* Fott and mass cultivation for oil production. *Algal Res.* 25, 142–148. <https://doi.org/10.1016/j.algal.2017.05.012>.
- Coates, J., 2006. Interpretation of Infrared Spectra, A Practical Approach. In: *Encyclopedia of Analytical Chemistry*. [10.1002/9780470027318.a5606](https://doi.org/10.1002/9780470027318.a5606).
- Corredor, L., Barnhart, E.P., Parker, A.E., Gerlach, R., Fields, M.W., 2021. Effect of temperature, nitrate concentration, pH and bicarbonate addition on biomass and lipid accumulation in the sporulating green alga *PW95*. *Algal Res.* 53, 102148. <https://doi.org/10.1016/j.algal.2020.102148>.
- Difusa, A., Talukdar, J., Kalita, M.C., Mohanty, K., Goud, V.V., 2015. Effect of light intensity and pH condition on the growth, biomass and lipid content of microalgae *Scenedesmus* species. *Biofuels* 6 (1–2), 37–44. <https://doi.org/10.1080/17597269.2015.1045274>.
- Do, C.V.T., Nguyen, N.T.T., Tran, T.D., Pham, M.H.T., Pham, T.Y.T., 2021. Capability of carbon fixation in bicarbonate-based and carbon dioxide-based systems by *Scenedesmus acuminatus* TH04. *Biochem. Eng. J.* 166, 107858. <https://doi.org/10.1016/j.bej.2020.107858>.
- Dubois, M., Gilles, K. A., Hamilton, J. K., Rebers, P. A., Smith, F., 1956. Colorimetric Method for Determination of Sugars and Related Substances. *Analy. Chem.* 10.1021/ac60111a017
- Faizal, A., Sembada, A.A., Priharto, N., 2021. Production of bioethanol from four species of duckweeds (*Landoltia punctata*, *Lemna aequinoctialis*, *Spirodela polyrrhiza*, and *Wolffia arrhiza*) through optimization of saccharification process and fermentation with *Saccharomyces cerevisiae*. *Saudi J. Biol. Sci.* 28 (1), 294–301. <https://doi.org/10.1016/j.sjbs.2020.10.002>.
- Feng, P., Deng, Z., Fan, L., Hu, Z., 2012. Lipid accumulation and growth characteristics of *Chlorella zofingensis* under different nitrate and phosphate concentrations. *J. Biosci. Bioeng.* 114 (4), 405–410. <https://doi.org/10.1016/j.jbiosc.2012.05.007>.
- Ferreira, G.F., Ríos Pinto, L.F., Carvalho, P.O., Coelho, M.B., Eberlin, M.N., Maciel Filho, R., Fregolente, L.V., 2019. Biomass and lipid characterization of microalgae genera *Botryococcus*, *Chlorella*, and *Desmodesmus* aiming high-value fatty acid production. *Biomass Convers. Biorefin.* 11 (5), 1675–1689. <https://doi.org/10.1007/s13399-019-00566-3>.
- Fields, F. J., Hernandez, R. E., Weibacher, E., Garcia-Vargas, E., Huynh, J., Thurmond, M., Lund, R., Burkart, M. D., Mayfield, S. P., 2021. Annual productivity and lipid composition of native microalgae (Chlorophyta) at a pilot production facility in Southern California. *Algal Research*, 56(September 2020), 102307. [10.1016/j.algal.2021.102307](https://doi.org/10.1016/j.algal.2021.102307)
- Fozer, D., Kiss, B., Lorincz, L., Szekely, E., Mizsey, P., Nemeth, A., 2019. Improvement of microalgae biomass productivity and subsequent biogas yield of hydrothermal gasification via optimization of illumination. *Renewable Energy* 138, 1262–1272. <https://doi.org/10.1016/j.renene.2018.12.122>.
- Fu, L., Cui, X., Li, Y., Xu, L., Zhang, C., Xiong, R., Zhou, D., Crittenden, J.C., 2017. Excessive phosphorus enhances *Chlorella regularis* lipid production under nitrogen starvation stress during glucose heterotrophic cultivation. *Chem. Eng. J.* 330 (August), 566–572. <https://doi.org/10.1016/j.cej.2017.07.182>.
- Gill, S.S., Mehmood, M.A., Ahmad, N., Ibrahim, M., Rashid, U., Ali, S., Nehdi, I.A., 2016. Strain selection, growth productivity and biomass characterization of novel microalgae isolated from fresh and wastewaters of upper Punjab, Pakistan. *Front. Life Sci.* 10.1080/21553769.2016.1204957
- Giordano, M., Kansiz, M., Heraud, P., Beardall, J., Wood, B., McNaughton, D., 2001. Fourier Transform Infrared spectroscopy as a novel tool to investigate changes in intracellular macromolecular pools in the marine microalga *Chaetoceros muellerii* (Bacillariophyceae). *J. Phycol.* 37 (2), 271–279. <https://doi.org/10.1046/j.1529-8817.2001.037002271.x>.
- Guldhe, A., Renuka, N., Singh, P., Bux, F., 2019. Effect of phytohormones from different classes on gene expression of *Chlorella sorokiniana* under nitrogen limitation for enhanced biomass and lipid production. *Algal Res.* 40, (March). <https://doi.org/10.1016/j.algal.2019.101518>.
- Hossain, M.N.B., Basu, J.K., Mamun, M., 2015. The production of ethanol from microalgae spirulina. *Proc. Eng.* 105, 733–738. <https://doi.org/10.1016/j.proeng.2015.05.064>.
- Huesemann, M., Crowe, B., Waller, P., Chavis, A., Hobbs, S., Edmundson, S., Wigmosta, M., 2016. A validated model to predict microalgae growth in outdoor pond cultures subjected to fluctuating light intensities and water temperatures. *Algal Res.* 13, 195–206. <https://doi.org/10.1016/j.algal.2015.11.008>.
- Joe, M.H., Kim, D.H., Choi, D.S., Bai, S., 2018. Optimization of phototrophic growth and lipid production of a newly isolated microalga, *desmodesmus* sp. KAERI-NJ5. *Microbiol. Biotechnol. Lett.* 46 (4), 377–389. <https://doi.org/10.4014/mbl.1808.08003>.

- John, D.M., Whitton, B.A., Brook, A.J. (n.d.). *The Flora is dedicated to John W.G. Lund FRS*.
- Khan, M.I., Shin, J.H., Kim, J.D., 2018. The promising future of microalgae: Current status, challenges, and optimization of a sustainable and renewable industry for biofuels, feed, and other products. In *Microbial Cell Factories* 17 (1). <https://doi.org/10.1186/s12934-018-0879-x>.
- Kim, E.J., Kim, S., Choi, H.G., Han, S.J., 2020. Co-production of biodiesel and bioethanol using psychrophilic microalga *Chlamydomonas* sp. KNM0029C isolated from Arctic sea ice. *Biotechnol. Biofuels*. <https://doi.org/10.1186/s13068-020-1660-z>.
- Kim, T.H., Lee, K., Oh, B.R., Lee, M.E., Seo, M., Li, S., Kim, J.K., Choi, M., Chang, Y.K., 2021. A novel process for the coproduction of biojet fuel and high-value polyunsaturated fatty acid esters from heterotrophic microalgae *Schizochytrium* sp. ABC101. *Renewable Energy* 165, 481–490. <https://doi.org/10.1016/j.renene.2020.09.116>.
- Klin, M., Pniewski, F., Latała, A., 2018. Characteristics of the growth rate and lipid production in fourteen strains of Baltic green microalgae. *Oceanol. Hydrobiol. Stud.* 47 (1), 10–18. <https://doi.org/10.1515/ohs-2018-0002>.
- Klin, M., Pniewski, F., Latała, A., 2020. Growth phase-dependent biochemical composition of green microalgae: Theoretical considerations for biogas production. *Bioresour. Technol.* 303, 122875. <https://doi.org/10.1016/j.biortech.2020.122875>.
- Kurano, N., Miyachi, S., 2005. Selection of microalgal growth model for describing specific growth rate-light response using extended information criterion. *J. Biosci. Bioeng.* 100 (4), 403–408. <https://doi.org/10.1263/jbb.100.403>.
- Lee, C.G., 1999. Calculation of light penetration depth in photobioreactors. *Biotechnol. Bioprocess Eng.* 4 (1), 78–81. <https://doi.org/10.1007/BF02931920>.
- Liu, J., Qiu, Y., He, L., Luo, K., Wang, Z., 2021. Effect of iron and phosphorus on the microalgae growth in co-culture. *Arch. Microbiol.* 203 (2), 733–740. <https://doi.org/10.1007/s00203-020-02074-9>.
- Lovio-Fragoso, J.P., Hayano-Kanashiro, C., López-Elías, J.A., 2019. Effect of different phosphorus concentrations on growth and biochemical composition of chaetoceros muelleri. *Latin Am. J. Aquatic Res.* 47 (2), 361–366. <https://doi.org/10.3856/vol47-issue2-fulltext-17>.
- Mayers, J.J., Vaiculyte, S., Malmhäll-Bah, E., Alcaide-Sancho, J., Ewald, S., Godhe, A., Ekendahl, S., Albers, E., 2018. Identifying a marine microalgae with high carbohydrate productivities under stress and potential for efficient flocculation. *Algal Res.* 31 (March), 430–442. <https://doi.org/10.1016/j.algal.2018.02.034>.
- Metsoviti, M.N., Papapolymerou, G., Karapanagiotidis, I.T., Katsoulas, N., 2019. Comparison of growth rate and nutrient content of five microalgae species cultivated in greenhouses. *Plants* 8 (8), 279. <https://doi.org/10.3390/plants8080279>.
- Miah, R., Siddiq, A., Tuli, J.F., Barman, N.K., Dey, S.K., Adnan, N., Yamada, M., Talukder, A.A., 2017. Inexpensive Procedure for Measurement of Ethanol: Application to Bioethanol Production Process. *Adv. Microbiol.* 07 (11), 743–748. <https://doi.org/10.4236/aim.2017.711059>.
- Miranda, C.T., de Lima, D.V.N., Atella, G.C., de Aguiar, P.F., Azevedo, S.M.F.O., 2016. Optimization of Nitrogen, Phosphorus and Salt for Lipid Accumulation of Microalgae: Towards the Viability of Microalgal Biodiesel. *Nat. Sci.* 10.4236/ns.2016.812055
- Morales-Sánchez, D., Schulze, P.S.C., Kiron, V., Wijffels, R.H., 2020. Temperature-Dependent Lipid Accumulation in the Polar Marine Microalga *Chlamydomonas malina* RCC2488. *Front. Plant Sci.* 11 (December), 1–10. <https://doi.org/10.3389/fpls.2020.619064>.
- Moreno-García, L., Gariépy, Y., Barnabé, S., Raghavan, G.S.V., 2019. Effect of environmental factors on the biomass and lipid production of microalgae grown in wastewaters. *Algal Res.* 41, (April). <https://doi.org/10.1016/j.algal.2019.101521>.
- Movasaghi, Z., Rehman, S., ur Rehman, D.I., 2008. Fourier transform infrared (FTIR) spectroscopy of biological tissues. In *Applied Spectroscopy Reviews* 43 (2), 134–179. <https://doi.org/10.1080/05704920701829043>.
- Mustapa, M., Sallehudin, N.J., Mohamed, M.S., Noor, N.M., Raus, R.A., 2016. Decontamination of *Chlorella* sp. Culture using antibiotics and antifungal cocktail treatment. *ARPN J. Eng. Appl. Sci.*
- Naghypour, D., Taghavi, K., Jaafari, J., Mahdavi, Y., Ghanbari Ghoskhal, M., Ameri, R., Jamshidi, A., Hossein Mahvi, A., 2016. Statistical modeling and optimization of the phosphorus biosorption by modified *Lemna minor* from aqueous solution using response surface methodology (RSM). *Desalin. Water Treat.* 57 (41), 19431–19442. <https://doi.org/10.1080/19443994.2015.1100555>.
- Naumann, D., Fabian, H., Lasch, P., 2009. FTIR spectroscopy of cells, tissues and body fluids. *Adv. Biomed. Spectroscopy*. <https://doi.org/10.3233/978-1-60750-045-2-312>.
- Özçimen, D., İnan, B., 2015. An Overview of Bioethanol Production From Algae. In *Biernat, K. (Ed.), Biofuels*. IntechOpen. 10.5772/59305
- Peng, X., Meng, F., Wang, Y., Yi, X., Cui, H., 2020. Effect of pH, Temperature, and CO<sub>2</sub> Concentration on Growth and Lipid Accumulation of *Nannochloropsis* sp. MASC 11. *J. Ocean Univ. China* 19 (5), 1183–1192. <https://doi.org/10.1007/s11802-020-4302-y>.
- Phwan, C.K., Ong, H.C., Chen, W.-H., Ling, T.C., Ng, E.P., Show, P.L., 2018. Overview: Comparison of pretreatment technologies and fermentation processes of bioethanol from microalgae. In *Energy Conversion and Management* 173, 81–94. <https://doi.org/10.1016/j.enconman.2018.07.054>.
- Piasecka, A., Nawrocka, A., Wiącek, D., Krzemińska, I., 2020. Agro-industrial by-product in photoheterotrophic and mixotrophic culture of *Tetrademus obliquus*: Production of ω<sub>3</sub> and ω<sub>6</sub> essential fatty acids with biotechnological importance. *Sci. Rep.* 10 (1). <https://doi.org/10.1038/s41598-020-63184-4>.
- Poh, Z.L., Amalina Kadir, W.N., Lam, M.K., Uemura, Y., Suparmaniam, U., Lim, J.W., Show, P.L., Lee, K.T., 2020. The effect of stress environment towards lipid accumulation in microalgae after harvesting. *Renewable Energy* 154, 1083–1091. <https://doi.org/10.1016/j.renene.2020.03.081>.
- Qiu, R., Gao, S., Lopez, P.A., Ogden, K.L., 2017. Effects of pH on cell growth, lipid production and CO<sub>2</sub> addition of microalgae *Chlorella sorokiniana*. *Algal Res.* 28 (December 2017), 192–199. <https://doi.org/10.1016/j.algal.2017.11.004>.
- Rismani-Yazdi, H., Haznedaroglu, B.Z., Bibby, K., Peccia, J., 2011. Transcriptome sequencing and annotation of the microalgae *Dunaliella tertiolecta*: Pathway description and gene discovery for production of next-generation biofuels. *BMC Genomics* 12 (1). <https://doi.org/10.1186/1471-2164-12-148>.
- Roopnarain, A., Gray, V.M., Sym, S.D., 2014. Phosphorus limitation and starvation effects on cell growth and lipid accumulation in *Isochrysis galbana* U4 for biodiesel production. *Bioresour. Technol.* 156, 408–411. <https://doi.org/10.1016/j.biortech.2014.01.092>.
- Sankaran, R., Show, P.L., Nagarajan, D., Chang, J.S., 2018. Exploitation and biorefinery of microalgae. In: *Waste Biorefinery: Potential and Perspectives*. 10.1016/B978-0-444-63992-9.00019-7
- Selvan, S.T., Govindasamy, B., Muthusamy, S., Ramamurthy, D., 2019. Exploration of green integrated approach for effluent treatment through mass culture and biofuel production from unicellular alga, *Acutodesmus obliquus* RDS01. *Int. J. Phytorem.* 21 (13), 1305–1322. <https://doi.org/10.1080/15226514.2019.1633255>.
- Stehfest, K., Toepel, J., Wilhelm, C., 2005. The application of micro-FTIR spectroscopy to analyze nutrient stress-related changes in biomass composition of phytoplankton algae. *Plant Physiol. Biochem.* 43 (7), 717–726. <https://doi.org/10.1016/j.plaphy.2005.07.001>.
- Sultana, N., Hossain, S.M.Z., Mohammed, M.E., Irfan, M.F., Haq, B., Faruque, M.O., Razzak, S.A., Hossain, M.M., 2020. Experimental study and parameters optimization of microalgae based heavy metals removal process using a hybrid response surface methodology-crow search algorithm. *Scientific Reports*. <https://doi.org/10.1038/s41598-020-72236-8>.
- Suthar, S., Verma, R., 2018. Production of *Chlorella vulgaris* under varying nutrient and abiotic conditions: A potential microalga for bioenergy feedstock. *Process Saf. Environ. Prot.* 113, 141–148. <https://doi.org/10.1016/j.psep.2017.09.018>.
- Tan, K.W.M., Lee, Y.K., 2016. The dilemma for lipid productivity in green microalgae: Importance of substrate provision in improving oil yield without sacrificing growth. *Biotechnol. Biofuels* 9 (1), 1–14. <https://doi.org/10.1186/s13068-016-0671-2>.
- Tang, C.Q., Leasi, F., Obertegger, U., Kieneker, A., Barraclough, T.G., Fontaneto, D., 2012. The widely used small subunit 18S rDNA molecule greatly underestimates true diversity in biodiversity surveys of the meiofauna. *PNAS* 109 (40), 16208–16212. <https://doi.org/10.1073/pnas.1209160109>.
- Turkcan, A., 2018. Effects of high bioethanol proportion in the biodiesel-diesel blends in a CRDI engine. *Fuel* 223, 53–62. <https://doi.org/10.1016/j.fuel.2018.03.032>.
- Yaakob, M.A., Mohamed, R.M.S.R., Al-Gheethi, A., Aswathnarayana Gokare, R., Ambati, R.R., 2021. Influence of Nitrogen and Phosphorus on Microalgal Growth, Biomass, Lipid, and Fatty Acid Production: An Overview. *Cells* 10 (2), 10–20. <https://doi.org/10.3390/cells10020393>.
- Yang, F., Long, L., Sun, X., Wu, H., Li, T., Xiang, W., 2014. Optimization of medium using response surface methodology for lipid production by *Scenedesmus* sp. *Mar. Drugs* 12 (3), 1245–1257. <https://doi.org/10.3390/md12031245>.
- Yang, Z., Pei, H., Han, F., Wang, Y., Hou, Q., Chen, Y., 2018. Effects of air bubble size on algal growth rate and lipid accumulation using fine-pore diffuser photobioreactors. *Algal Res.* 32 (March), 293–299. <https://doi.org/10.1016/j.algal.2018.04.016>.
- Yanuar, U., Caesar, N.R., Musa, M., 2019. Identification of Local Isolate of Microalgae *Chlorella Vulgaris* using Ribulose-1,5-Bisphosphate Carboxylase/Oxygenase Large Subunit (rbcL) Gene. *IOP Conference Series: Materials Science and Engineering* 546, 022038. <https://doi.org/10.1088/1757-899X/546/2/022038>.
- Yun, H.-S., Lee, H., Park, Y.-T., Ji, M.-K., Kabra, A.N., Jeon, C., Jeon, B.-H., Choi, J., 2014. Isolation of novel microalgae from acid mine drainage and its potential application for biodiesel production. *Appl. Biochem. Biotechnol.* 173 (8), 2054–2064. <https://doi.org/10.1007/s12010-014-1002-3>.
- Yusuf, A.A., Inambao, F.L., 2021. Effect of low bioethanol fraction on emissions, performance, and combustion behavior in a modernized electronic fuel injection engine. *Biomass Convers. Biorefin.* 11 (3), 885–893. <https://doi.org/10.1007/s13399-019-00519-w>.
- Zhang, Y., Ren, L., Chu, H., Zhou, X., Yao, T., Zhang, Y., 2019. Optimization for *Scenedesmus obliquus* Cultivation: The effects of temperature, light intensity and pH on growth and biochemical composition. *Microbiol. Biotechnol. Lett.* 47 (4), 614–620. <https://doi.org/10.4014/mbl.1906.06005>.